Transition State Analysis and Requirement of Asp-262 General Acid/Base Catalyst for Full Activation of Dual-Specificity Phosphatase MKP3 by Extracellular Regulated Kinase†

Johanna D. Rigas,‡ Richard H. Hoff,§ Adrian E. Rice,‡ Alvan C. Hengge,§ and John M. Denu*,‡

Department of Biochemistry and Molecular Biology, Oregon Health Sciences University, Portland, Oregon 97201-3098, and Department of Chemistry and Biochemistry, Utah State University, Logan, Utah 84322-0300

Received December 28, 2000; Revised Manuscript Received February 16, 2001

ABSTRACT: Dual-specificity phosphatase MKP3 down-regulates mitogenic signaling through dephosphorylation of extracellular regulated kinase (ERK). Unlike a simple substrate−enzyme interaction, the noncatalytic, amino-terminal domain of MKP3 can bind efficiently to ERK, leading to activation of the phosphatase catalytic domain by as much as 100-fold toward exogenous substrates. It has been suggested that ERK activates MKP3 through the stabilization of the active phosphatase conformation, enabling general acid catalysis. Here, we investigated whether Asp-262 of MKP3 is the bona fide general acid and evaluated its contribution to the catalytic steps activated by ERK. Using site-directed mutagenesis, pH rate and Brönsted analyses, kinetic isotope effects, and steady-state and rapid reaction kinetics, Asp-262 was identified as the authentic general acid catalyst, donating a proton to the leaving group oxygen during P−O bond cleavage. Kinetic isotope effects [$^{18}(V/K)_{bridge}$, $^{18}(V/K)_{nonbridge}$, and $^{15}(V/K)$] were evaluated for the effect of ERK and of the D262N mutation on the transition state of the phosphoryl transfer reaction. The patterns of the three isotope effects for the reaction with native MKP3 in the presence of ERK are indicative of a reaction where the leaving group is protonated in the transition state, whereas in the D262N mutant, the leaving group departs as the anion. Even without general acid catalysis, the D262N mutant reaction is activated by ERK through increased phosphate affinity (∼8-fold) and the partial stabilization of the transition state for phospho-enzyme intermediate formation (∼4-fold). Based on these analyses, we estimate that dephosphorylation of phosphorylated ERK by the D262N mutant is >1000-fold lower than by native, activated MKP3. Also, the kinetic results suggest that Asp-262 functions as a general base during thiol−phosphate intermediate hydrolysis.

Dual-specificity phosphatases (DSPs)[1] are important regulators of cell-cycle control and mitogenic signal transduction. Compared with protein tyrosine phosphatases (PTPs), which share the active-site motif HCxxGxxR(S/T), DSPs can be distinguished by their ability to bind to and hydrolyze phosphotyrosine and phosphothreonine/serine residues that are often located in close proximity on the target protein. Many DSPs act as negative regulators of the mitogen-activated protein (MAP) kinases (*1*) which are activated by specific upstream dual-specificity kinases (MAP-kinase kinases, MKKs) through phosphorylation on threonine and tyrosine residues in the TxY motif. MAP kinases function to mediate intracellular signaling events triggered by mitogens, growth factors, and stress (*2, 3*). Specific DSPs have been shown to dephosphorylate both Thr and Tyr in the TxY motif of the various families of MAP kinases (*4*−*7*). Due to their specific dephosphorylation of MAP kinases, many of these DSPs have been termed MAP kinase phosphatases (MKPs) (*7*−*10*). One of the most intriguing enzymes is MKP3 (*8*) [also named rVH6 (*11*) and Pyst1 (*7*)]. Upon binding its proposed MAP kinase substrate, ERK, the enzyme displays up to a 100-fold activation in phosphatase activity against artificial substrates (*12, 13*). Interestingly, the tight binding and activation appear to be mediated through the N-terminal "noncatalytic" region of MKP3. This N-terminal region is likely a distinct domain from the C-terminal catalytic core and is not absolutely required for basal phosphatase activity. Catalytic activation of other members of the MKPs has also been observed (*1, 12, 14*), suggesting that substrate activation may be a general regulatory mechanism for these phosphatases.

Although a 3-dimensional structure of the N-terminal half of the MKPs has not been solved, recent biochemical data have implicated the importance of the region surrounding Arg-64 and Arg-65 (MKP3 residues) for ERK binding (*15*). A more recent report suggests that multiple protein−protein contacts are made between ERK and MKP3 (*16*). Also, the

† This work was supported by American Cancer Society Grant RPG-97-175-01-TBE and by NIH Grant GM59785 to J.M.D. and NIH Grant GM47297 to A.C.H.

* Correspondence should be addressed to this author at the Department of Biochemistry and Molecular Biology, Oregon Health Sciences University, 3181 SW Sam Jackson Park Rd., Portland, OR 97201-3098. Phone: (503) 494-0644. Fax: (503) 494-8393. E-mail: denuj@ohsu.edu.

‡ Oregon Health Sciences University.

§ Utah State University.

[1] Abbreviations: ERK, extracellular regulated kinase; PTP, protein tyrosine phosphatase; DSP, dual-specificity phosphatase; *p*NPP, *p*-nitrophenyl phosphate; *p*NP, *p*-nitrophenol; Bis-Tris, [bis(2-hydroxyethyl)amino]tris(hydroxymethyl)methane.

10.1021/bi002951v CCC: $20.00
Published on Web 03/16/2001

interacting portions of ERK have been mapped near Asp-321 and Asp-324 (*17*). However, how these relatively distant interactions induce the catalytic activation within the C-terminal phosphatase domain is unknown.

When the X-ray structure for the catalytic domain of Pyst1-(MKP3) was recently reported, it was noted that the overall structure was similar to the previously published X-ray structure of the DSP VHR (*18*). The full-length structure of VHR (*19*) represents the putative catalytic domain shared with these larger DSPs, such as MKP3 (~30% sequence identity within the catalytic domain). VHR has served as the prototypical model DSP for detailed biochemical, structural, and catalytic studies (*19*−*25*). The nucleophilic thiolate of cysteine-124 in the signature motif attacks the phosphorus of substrate, transferring the phosphate group to the enzyme and forming a cysteinyl−phosphate intermediate. On a separate loop structure known to be flexible in several PTPs, conserved aspartic acid-92 facilitates catalysis by protonating the leaving group oxygen. With MKP3, substrate binding is thought to induce the movement of the "general acid loop" toward the active site such that the conserved aspartic acid is in position to transfer a proton to the leaving group. In the Pyst1 X-ray structure (*18*), the proposed "general acid loop" was flipped 20 Å away from the active-site cleft, suggesting that the putative general acid (Asp-262) could not participate in catalysis. We have recently suggested that ERK binding to MKP3/Pyst1/rVH6 induces general acid loop closure and the subsequent involvement of general acid catalysis, as well as ground state and transition state stabilization (*13*). Similar proposals have been suggested by others (*18*, *26*). However, direct biochemical and kinetic evidence that Asp-262 is the authentic general acid catalyst was lacking. This would be a significant finding since recent work with the cdc25 dual-specificity phosphatase has suggested that its protein kinase substrate, Cdk2, may provide the general acid during catalysis (*27*). Several proposed carboxylate-containing residues of cdc25 that had been implicated in general acid catalysis were ruled out as candidates (*27*). Also, evidence that Asp-262 in MKP3 was directly contributing to the dramatic activation of MKP3 remained to be established.

To provide direct evidence for the role of Asp-262 during ERK-dependent and -independent catalytic activation, we have performed an extensive enzymatic comparison of the activated and unactivated D262N mutant of MKP3. Using steady-state and rapid reaction kinetics, pH studies, kinetic isotope effects, and Brönsted analysis, we demonstrate that Asp-262 is the general acid catalyst. Also, we have determined that the D262N enzyme was still capable of being activated by ERK ~20−30-fold. This residual activation results from increased phosphate binding affinity and transition state stabilization. We have previously used heavy atom isotope effects to characterize the transition states of the reaction of *p*-nitrophenyl phosphate (*p*NPP) catalyzed by VHR, a prototype of the DSP family. In the present study, we have sought to examine the effect of the activator ERK on the structure of the transition state of the phosphoryl transfer reaction in native MKP3, and in the mutant D262N.

MATERIALS AND METHODS

Reagents and Enzymes. Chemicals were of the highest grade commercially available. MKP3 and ERK were expressed and purified as described in refs *28* and *29*, respectively. The 8-difluoro-4-methylumbelliferyl phosphate substrate (*13*, *30*) was obtained from Molecular Probes (Eugene, OR). The D262N mutant was generated by single oligonucleotide site-directed mutagenesis, as described previously (*22*). The mutation was confirmed by DNA sequencing.

Synthesis of Compounds. Natural-abundance *p*-nitrophenyl phosphate, [^{14}N]-*p*-nitrophenyl phosphate, [^{15}N, nonbridge-$^{18}O_3$]-*p*-nitrophenyl phosphate, [^{14}N]-*p*-nitrophenol, and [^{15}N, ^{18}O]-*p*-nitrophenol were synthesized as described previously (*31*). [^{14}N]-*p*-Nitrophenol and [^{15}N, ^{18}O]-*p*-nitrophenol were then mixed to reconstitute the natural abundance of ^{15}N, and then the mixture was phosphorylated to produce *p*-nitrophenyl phosphate using the same method as referred to above. This mixture was used for determination of $^{18}(V/K)_{bridge}$. The [^{14}N]-*p*-nitrophenyl phosphate and [^{15}N, nonbridge-$^{18}O_3$]-*p*-nitrophenyl phosphate were also mixed to reconstitute the natural abundance of ^{15}N. This mixture was used for determination of $^{18}(V/K)_{nonbridge}$. The isotopic abundance of the mixtures was determined by isotope ratio mass spectrometry.

Assays. As described previously (*13*), assays were performed in a three-component system (constant ionic strength of 0.1 M) consisting of 0.1 M acetate, 0.05 M Tris [tris-(hydroxymethyl)aminomethane], and 0.05 M Bis-Tris ([bis-(2-hydroxyethyl)amino]tris(hydroxymethyl)methane). Increases in buffer concentration had no significant effect on the rates of catalysis, suggesting that our buffer was not acting as an alternate phosphate acceptor. Kinetic parameters k_{cat} and V/K were determined from the substrate concentration dependence of the initial velocities (eq 1). The pH profiles for k_{cat} and V/K were generated by determining these steady-state parameters at the indicated pH values. Increasing the level of ERK to MKP3 above a ratio of 2:1 (i.e., 4:1) had no significant effect on the kinetic activation of MKP3 at the pH extremes (5.5 and 10), ensuring that complete ERK/MKP3 complex formation was achieved with a molar ratio of 2:1 over the entire pH range tested. The pH profiles were fitted to eqs 2 and 3, depending upon the shape of the profile. Fitting of the pH-dependent data to eqs 2 and 3 was accomplished with nonlinear least-squares fitting using the computer program Kaleidagraph (Abelbeck Software) for Macintosh. In eqs 2 and 3, C (or C_1, C_2) is the pH-independent value of either k_{cat} or V/K; H is the proton concentration; K_a, K_b, and K_c are the ionization constants.

$$v = [E]_0 k_{cat} S/(S + K_m) \quad (1)$$

$$v = C/[(1 + H/K_a)(1 + H/K_c)] \quad (2)$$

$$v = \{(C_1/(((1.0 + (1 + H/K_a))(1.0 + (1 + H/K_c)))) + (C_2(1 + K_b/H)))/(1 + (1 + K_b/H))\} \quad (3)$$

Inhibition by Phosphate. The inhibition constant K_i of MKP3 for phosphate was determined as previously described (*13*). Inhibition was competitive with respect to the substrate *p*NPP, and eq 4 was used to calculate the inhibition constant.

$$v = V_{max} S/[K_m(1 + I/K_i) + S] \quad (4)$$

Leaving Group Dependence. The substrates *o*MFP (3-*o*-methylfluorescein phosphate) (pK_a = 4.6), 6,8-difluoro-4-

methylumbelliferyl phosphate ($pK_a = 4.7$), 8-fluoro-4-methylumbelliferyl phosphate ($pK_a = 6.4$), *p*NPP (*p*-nitrophenyl phosphate) ($pK_a = 7.1$), 4-methylumbelliferyl phosphate ($pK_a = 7.8$), β-naphthyl phosphate ($pK_a = 9.38$), and phenyl phosphate ($pK_a = 9.99$) were used and assayed as described previously (*13*). The k_{cat} and V/K values were determined from fits to eq 1.

Rapid Reaction Kinetics. The stopped-flow experiments were performed as described in ref *13*. Briefly, enzyme and substrate were rapidly mixed at 25 °C in a temperature-controlled SF-61 Hi-Tech Scientific (Hi-Tech Ltd, Salisbury, U.K.) stopped-flow spectrophotometer. Product formation of *p*-nitrophenol was monitored at 410 nm, 3-*o*-methylfluorescein at 477 nm, 6,8-difluoro-4-methylumbelliferone at 360 nm, 8-fluoro-4-methylumbelliferone at 360 nm, and 4-methylumbelliferone at 370 nm. Data were fitted to eq 5 using nonlinear least-squares analysis, where A is the amplitude of the burst, k is the first-order rate constant of product burst, B is the slope of the linear portion of the curve, C is the intercept of the line, and t is time.

$$\text{absorbance} = Ae^{-kt} + Bt + C \quad (5)$$

The burst rate was determined as a function of substrate concentration. Because the burst phase ($\sim k_3$) and the linear phase ($\sim k_5$) were well-resolved, the burst rates, k_{burst}, could be fitted to eq 6. The resulting ($k_3 + k_5$) value from eq 6 simplifies to k_3 since $k_3 \gg k_5$. All of the data displayed simple saturation kinetics as defined by eq 1 and by eq 6.

$$k_{burst} = (k_3 + k_5)[S]/(K_d + [S]) \quad (6)$$

Dephosphorylation of Phospho-ERK by MKP3 and D262N Mutant. Recombinant phosphorylated ERK (*32*) at a final concentration of 1 μM was combined with 2 μM recombinant wild-type MKP3 or MKP3 mutant D262N in 20 mM HEPES, pH 7.4, containing 10 mM $MgCl_2$. Reactions were incubated at 30 °C for the indicated times, up to 30 min, before quenching into 5× Laemmli sample buffer. The phosphorylation state of ERK was determined using SDS−PAGE and western analysis with an antibody that recognizes phosphorylated ERK (*32*).

Isotope Effect Determinations. Isotope effect determinations were made at 30 °C, pH 7.0 (100 mM Bis-Tris/Tris), 1 mM DTT. The protocols for carrying out these experiments were the same as those previously described (*25*). In this method, the enzymatic reactions are allowed to proceed to partial completion and stopped, followed by separation of the product and residual substrate. These are then subjected to isotopic analysis by isotope ratio mass spectrometry to determine the isotope effect. Isotopic analyses were performed using an ANCA-NT combustion system in tandem with a Europa 20-20 isotope ratio mass spectrometer. Reactions were begun with 100 μmol or more of the substrate, and sufficient enzyme, or enzyme with ERK, was added so that the background hydrolysis rate was negligible compared to the enzymatic reaction. Parallel experiments without enzyme were used to establish background hydrolysis rates under the experimental conditions.

Isotope effects were calculated from the isotopic ratio of the *p*-nitrophenol product at partial reaction (R_p), in the residual substrate (R_s), and in the starting material (R_o). Equations 7 and 8 were used to calculate the observed isotope effect either from R_p and R_o or from R_s and R_o, respectively, at fraction of reaction f (*33*). Thus, each experiment yields two independent determinations of the isotope effect.

$$\text{isotope effect} = \log (1 - f)/\log [1 - f(R_p/R_o)] \quad (7)$$

$$\text{isotope effect} = \log (1 - f)/\log [(1 - f)(R_s/R_o)] \quad (8)$$

R_o was determined separately from unreacted substrate by isotope ratio mass spectroscopic analysis and, as a control, from *p*-nitrophenol isolated after complete hydrolysis of substrate using the isolation and purification procedures used in the isotope effect experiments. The agreement of these two numbers demonstrated that, within experimental error, no isotopic fractionation occurs as a result of the procedures used to isolate and purify the *p*-nitrophenol.

The ^{18}O isotope effects were measured by the remote-label method (*34*), as previously described for the solution reactions of *p*NPP (*31*). In these experiments, the nitrogen atom in the substrate is used as a reporter for isotopic changes at the bridging oxygen atom or the nonbridging oxygen atoms. These experiments yield an observed isotope effect, which is the product of the effect due to ^{15}N and to ^{18}O substitutions. The observed isotope effects from these experiments were then corrected for the ^{15}N effect and for incomplete levels of isotopic incorporation in the starting material as previously described (*35*).

The notation used to express isotope effects is that of Northrop (*36*) where a leading superscript of the heavier isotope is used to indicate the isotope effect on the following kinetic quantity; for example, ^{15}k denotes k_{14}/k_{15}, the nitrogen-15 isotope effect on the rate constant k. Figure 7 shows a diagram of the substrate with the nomenclature used to describe the isotope effects at each position. Since the enzymatic isotope effects in this study were measured by the competitive method, they are isotope effects on V/K, and thus are designated as $^{15}(V/K)$, etc. Thus, the isotope effects reveal the first phosphoryl transfer step, from the substrate to the enzymatic nucleophile cysteine.

RESULTS AND DISCUSSION

It has been suggested previously that activation of MKP3 by ERK involves the recruitment of a general acid catalyst, and that native MKP3 is incapable of efficient general acid catalysis (*13*). Asp-262 has been suggested to be the general acid group in MKP3 (*13*, *18*, *28*), but this has not been demonstrated directly. Other possibilities could exist. For instance, a recent paper on the DSP cdc25 has suggested that the general acid does not arise from the phosphatase, but, rather, may come from its protein substrate cdk2 (*27*). To resolve whether the general acid group resides on MKP3 and whether D262 is the authentic general acid, we created the D262N mutant of MKP3 and probed the role of D262 in catalysis by ERK-activated MKP3.

The hallmark of DSP and PTP pH profiles is a bell-shaped curve where the nucleophile cysteine must be unprotonated, the general acid aspartic acid must be protonated, and the substrate must be unprotonated during phosphoryl transfer to the enzyme (*37* and Figure 1). Cysteine is the acceptor of the phosphate group from substrate, forming a thiol−phosphate intermediate. The conserved aspartic acid donates

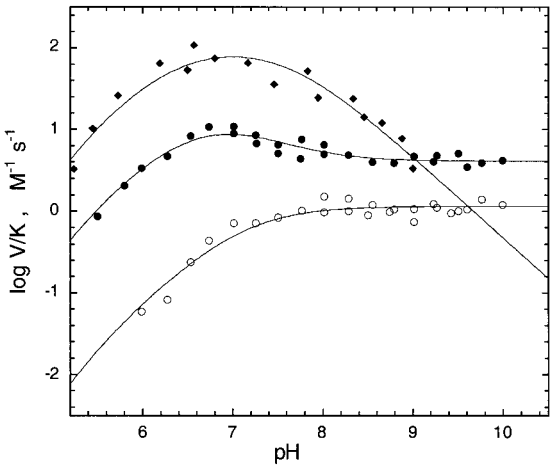

FIGURE 1: Effect of pH on the *V*/*K* value for ERK-activated and unactivated MKP3 mutant D262N. The D262N mutant was activated by ERK protein added at 2× the concentration of MKP3. The unactivated pH profile (open circles) of *V*/*K* was fitted to eq 2, and the ERK-activated pH profile (filled circles) was fitted to eq 3. For comparison, previously determined data (*13*) from ERK-activated native MKP3 are displayed (filled diamonds). Conditions: 0.1 M sodium acetate, 0.05 M Tris, and 0.05 M Bis-Tris, 25 °C.

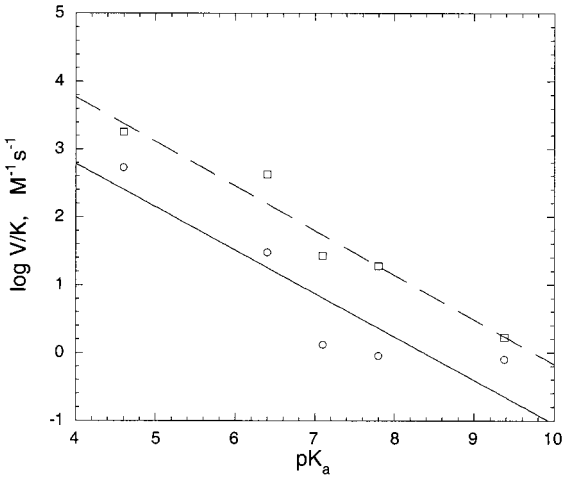

FIGURE 2: Effect of substrate leaving group pK_a value on the *V*/*K* value of activated and unactivated MKP3 mutant D262N. Open circles indicate unactivated D262N, and open squares indicate ERK-activated D262N. Substrates 6,8-difluoro-4-methylumbelliferyl phosphate (pK_a = 4.7), 8-fluoro-4-methylumbelliferyl phosphate (pK_a = 6.4), *p*NPP (pK_a = 7.1), 4-methylumbelliferyl phosphate (pK_a = 7.8), β-naphthyl phosphate (pK_a = 9.38), and phenyl phosphate (pK_a = 9.99) were used and assayed as described previously (*13*). Data were fitted using linear least-squares regression. Conditions: pH 7 and 25 °C.

a proton to the leaving group oxygen to facilitate P−O bond cleavage. Previously, native MKP3 was shown to lack efficient general-acid-catalyzed monoester hydrolysis (*13, 28*) while ERK-activated MKP3 clearly exhibited general acid catalysis (*13*). In part, this conclusion was based upon the appearance of a critical ionization that must be protonated for activity. The pH profile of the low-activity native enzyme did not display this critical ionization.

pH Rate Analysis. The D262N mutant was subjected to pH rate analysis to probe the involvement of general acid catalysis during activation by ERK, and to identify D262 as the authentic general acid catalyst. Initially, the D262N mutant was analyzed in the absence of ERK protein. The apparent second-order rate constant *V*/*K* was determined for the general phosphatase substrate *p*NPP as a function of pH. The *V*/*K* parameter describes the reaction between free enzyme and free substrate, and will reflect important ionizations involved for both substrate binding and catalysis. The D262N mutant exhibited two ionizations for groups that must be unprotonated, but no ionization for a group that must be protonated for activity. The two unprotonated groups have been previously assigned to *p*NPP (pK_a = 5.1) and the catalytic cysteine (pK_a = 6.5) (*13*). Interestingly, the D262N mutant displays a *V*/*K* optimum value of 2.75 M^{-1} s^{-1}, which is only 2.3-fold lower than the native enzyme (without ERK). Similarly, the pH profile of the D262N mutant in the presence of ERK protein exhibited no critical ionization for a group that must be protonated for activity,[2] consistent with the hypothesis that D262 is the general acid catalyst. However, to our surprise, ERK was still able to induce an ~10-fold enhancement in the *V*/*K* rate constant. These data suggested that although general acid catalysis could be abolished, the D262N mutant could still be significantly activated by ERK throughout the entire pH range investigated (pH 6−10). The pH dependence of k_{cat} was also determined; but, due to an inability to saturate at low pH and obtain significant initial velocities, k_{cat} values could not be accurately obtained below pH 7. Nonetheless, above pH 7, k_{cat} values (0.002−0.003 s^{-1}) were nearly identical between D262N and ERK-activated D262N. In contrast to activated wild-type MKP3, both D262N and ERK-activated D262N displayed no k_{cat} pH dependence in this range. Collectively, these data suggest that D262 is the authentic general acid catalyst responsible for the critical protonated group observed in the activated MKP3 pH profiles. In addition, our data suggested that induced general acid involvement cannot fully account for the residual activation by ERK.

Effect of Leaving Group pK_a Value. To provide evidence that D262 is the general acid, a Brönsted analysis was performed with the D262N mutant in the presence and absence of ERK. The *V*/*K* value was determined as a function of the leaving group pK_a value (4.6−9.4) for a variety of small molecule phosphate monoesters (Figure 2). The *V*/*K* value for D262N (±ERK) displayed a dramatic effect on the leaving group pK_a value, with similar slopes of −0.66 ± 0.09 and −0.64 ± 0.17 for ERK-activated and unactivated D262N, respectively. This result is in stark contrast to the previous observation that ERK-activated MKP3 exhibited no significant dependence on *V*/*K* or k_{cat} values (*13*). A strong dependence of the rate on the leaving group pK_a value has been an excellent diagnostic for the low efficiency, or lack of general-acid-facilitated P−O bond cleavage in PTP catalysis (*13, 38, 39*). We had previously demonstrated that MKP3's *V*/*K* value displays a strong dependence on leaving group pK_a value, while this effect was nearly ablated in the ERK-activated enzyme (*13*). The k_{cat} values for the D262N mutant exhibited a more complex, biphasic response to leaving group pK_a value (Figure 3). This was observed whether ERK was present. Between pK_a's of 4.6 and 6.4, there was little leaving group dependence; but above pK_a

[2] A nonessential ionization was observable in the ERK-activated D262N pH profile. However, this ionization was not critical since protonation of this group increased the *V*/*K* value ~5-fold. This ionization likely reflects a structural ionization that alters the maximal activation induced by ERK binding.

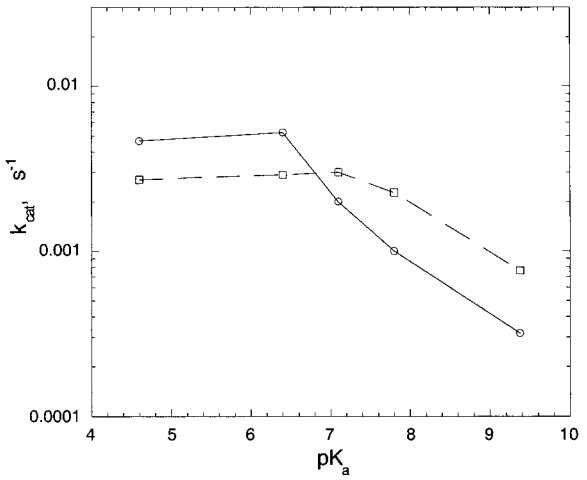

FIGURE 3: Effect of substrate leaving group pK_a value on the k_{cat} value of activated and unactivated MKP3 mutant D262N. Open circles indicate unactivated D262N, and open squares indicate ERK-activated D262N. See Figure 2 legend for substrate employed. Conditions: pH 7 and 25 °C.

Scheme 1: Kinetic Mechanism for DSP Catalysis

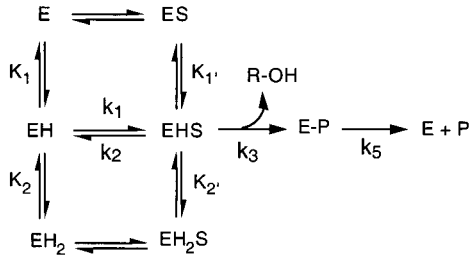

values of 7, there was a substantial dependence on the leaving group pK_a value, so that for every pK_a unit above 7 there was an ~5-fold decrease in k_{cat} value. These data suggest that there is an alteration in the rate-limiting step for catalysis when the leaving group pK_a is altered. This change occurs near a pK_a value of 7−8. Given the previously deduced kinetic mechanism (Scheme 1) for the DSPs VHR (*24*) and MKP3 (*13*), it is likely that turnover (k_{cat}) in the D262N mutant is limited by hydrolysis of the thiol−phosphate intermediate with substrates whose leaving group pK_a values are less than 7−8, but limited by P−O bond cleavage when the leaving group pK_a is higher than 7−8.

Rapid Reaction Kinetics. To provide more direct evidence for the role of D262 during catalysis, and to establish the rate-limiting step, stopped-flow rapid kinetics were performed. Using this analysis, the rate of P−O bond cleavage (k_3, see Scheme 1) can be extracted from the burst phase of the biphasic kinetic trace. However, this requires that intermediate hydrolysis (k_5) is slow relative to intermediate formation (k_3) (Scheme 1). Previously, this approach has been successfully applied to the study of VHR (*24*, *39*) and native MKP3 (*13*). Here, D262N in the presence or absence of a 2× molar excess of ERK was rapidly reacted with *p*NPP. Indeed, a burst phase followed by a slower linear phase was observed (kinetic traces not displayed). The kinetic trace was fitted to eq 5 as previously described (*13*), yielding the apparent first-order rate (k_{burst}) of the exponential burst at a given *p*NPP concentration. Kinetic traces at several substrate concentrations were collected, the resulting traces were fitted (eq 6), and the k_{burst} values were plotted as a function of *p*NPP concentration (Figure 4). The saturation curves

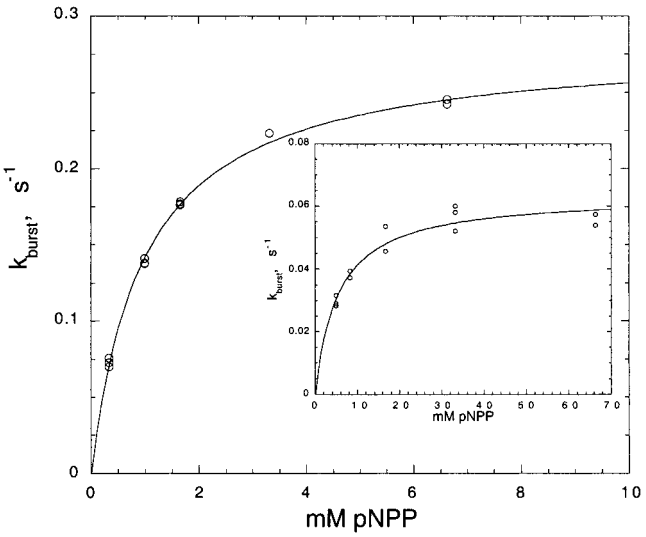

FIGURE 4: Rapid kinetics of MKP3 mutant D262N reacting with *p*NPP. Concentration dependence of k_{burst} for ERK-activated and unactivated (inset) D262N enzyme. The substrate saturation dependence of the raw kinetic traces was analyzed as described under Materials and Methods. In addition to *p*NPP, the substrates 6,8-difluoro-4-methylumbelliferyl phosphate (pK_a = 4.7), 8-fluoro-4-methylumbelliferyl phosphate (pK_a = 6.4), and 4-methylumbelliferyl phosphate (pK_a = 7.8) were analyzed by the identical approach. Resulting saturation curves were fitted using eq 1. Conditions: pH 7, 25 °C. [ERK] was maintained at 2× the [D262N], which ranged from 3 to 10 μM.

exhibited simple saturating kinetics (Figure 4) and therefore were fitted to the Michaelis−Menten equation to obtain the maximum rate of P−O bond cleavage, k_3. Rates from the linear phase exhibited the same steady-state values derived from separate steady-state kinetic analysis. The D262N rate constant for P−O bond cleavage (k_3) was 0.064 s^{-1}, compared with 0.281 s^{-1} in the presence of ERK. This represents a 4.4-fold rate enhancement, indicating significant transition state stabilization.

The pre-steady-state analysis was expanded to include substrates with differing leaving group pK_a values. Burst kinetics were observed for substrates whose leaving group pK_a values were less than 7.8, consistent with a transition in the rate-limiting step near this pK_a value. The occurrence of a product burst requires that enzyme intermediate breakdown (k_5) be at least partially limiting in turnover. The maximum k_{burst} rate was determined (as in Figure 4) for all substrates exhibiting burst kinetics, and was plotted in Figure 5 as a function of leaving group pK_a value. As predicted from a lack of general acid catalysis, the Brönsted plots (±ERK) displayed a large leaving group pK_a dependence, yielding a slope of −0.78 ± 0.12 for D262N and −0.91 ± 0.06 for D262N with ERK. For comparison, the previously obtained ERK-activated native MKP3 data are displayed in Figure 5. These results support the idea that the D262N mutant is incapable of protonating the leaving group oxygen and neutralizing the developing negative charge developed during the transition state for P−O cleavage. This effect is seen whether ERK is present, clearly ruling out the idea that ERK provides the general acid. This finding is especially relevant in light of the conclusion by Chen et al., who had suggested that general acid catalysis by the DSP cdc25 is provided by its kinase substrate Cdk2 (*27*). In the presence of ERK, it is also important to point out that with the higher leaving group

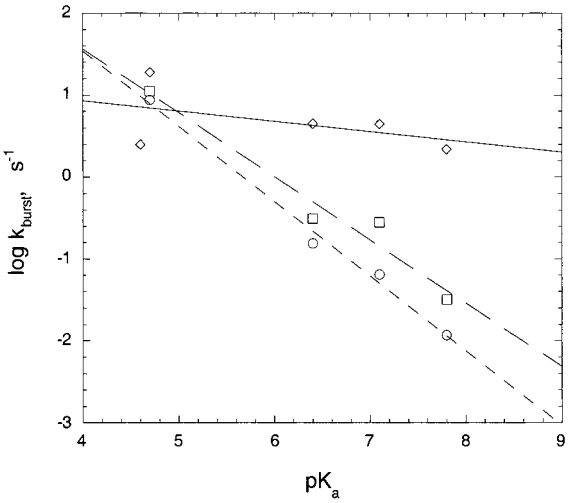

FIGURE 5: Effect of leaving group pK_a value on the rate of intermediate formation (k_3) for ERK-activated and unactivated D262N. The k_3 value was determined (see Figure 4) as a function of leaving group pK_a. Open squares represent D262N with ERK, while open circles represent unactivated D262N. For comparison, previously determined data (*13*) from ERK-activated native MKP3 are displayed (open diamonds). Lines are the best fits to linear least-squares regression analysis. Conditions: pH 7 and 25 °C.

Scheme 2: MKP3 Catalytic Mechanism for Phosphoryl-enzyme Intermediate Formation

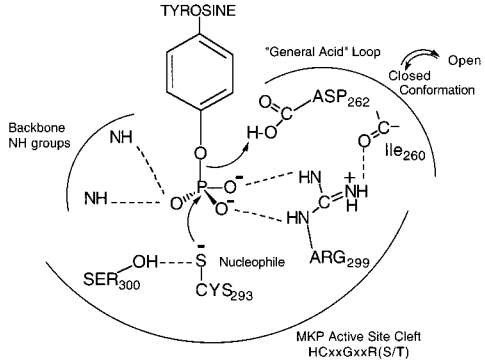

pK_a values examined, the D262N mutant displays a slightly (2−4-fold) faster rate (Figure 5). As we have proposed, ERK may activate MKP3 by inducing closure of the general acid loop (Scheme 2). The significant but small effect of ERK on k_3 could be due to a stabilizing effect of Asn at position 262, since this residue is still capable of hydrogen-bonding to the leaving group oxygen. Alternatively, the additional rate enhancement could be the consequence of ERK inducing general acid loop closure and correctly positioning Arg-299 for transition state stabilization of the phosphate oxygens. In the distantly related *Yersinia* PTP, general acid loop movement is required to properly position the conserved arginine residue (*40*). Also, mutations on the general acid loop affect the ability of the general acid to efficiently participate in catalysis (*40*). We had previously suggested that ERK-induced general acid loop closure can increase oxyanion affinity by properly positioning Arg-299 through hydrogen bonding to the carbonyl oxygen of Ile-260 on the general acid loop (*13*).

Effect of ERK-Induced Activation on MKP3 Substrate Binding. The *V*/*K* second-order rate constant for D262N displays the largest increase (>10-fold) of any kinetic parameter investigated (i.e., k_{cat} or k_3) when this mutant is activated by ERK. The k_{cat} value is equal to $k_3k_5/(k_3 + k_5)$. Because the *V*/*K* value $[k_1k_3/(k_2 + k_3)]$ involves both substrate binding and catalysis, we examined whether a major portion of the rate enhancement still remaining in the D262N mutant may be due to an increase in substrate affinity. To offer support for the increased substrate/ligand binding affinity of the ERK-activated D262N mutant, the dissociation constant (K_i) for phosphate was determined with and without ERK. D262N alone displayed a K_i of 14.2 ± 1.21 mM, whereas ERK-activated D262N exhibited a K_i of 1.68 ± 0.28 mM, representing more than 8-fold tighter phosphate binding. If we assume that the *V*/*K* value with *p*NPP is approximated by k_3/K_d (where $K_d = k_2/k_1$), a reasonable assertion with the catalytic D262N mutant, then the observed 20−30-fold higher *V*/*K* value (at pH 7 with *p*NPP) can be resolved into an 8-fold increase in K_d and a 4-fold increase in k_3. The calculated combined effect of ∼32-fold is in good agreement with the 20−30-fold effect on *V*/*K* under these conditions. Moreover, these observations strongly suggest that the D262N mutant is dysfunctional only in its ability to act as general acid/base, not in the enzyme's ability to correctly form the active phosphatase conformation. This argument rules out the idea that D262 plays a role in simply mediating the switch between the low- and high-activity forms of the enzyme.

We have previously demonstrated that addition of up to 25% DMSO can mimic the activation by ERK (*13*). We surmised that this effect was the result of DMSO acting as a chemical chaperone and stabilizing the closed conformation of the general acid loop (*13*). To demonstrate that the D262N mutant can be stabilized by DMSO and therefore mimic the remaining activation observed with ERK, *p*NPP substrate saturation curves with D262N were generated in the presence of 25% DMSO (pH 7 and 25 °C). The resulting saturation curves demonstrated an increase of 17-fold for the *V*/*K* value (1.32 M^{-1} s^{-1} versus 22.9 M^{-1} s^{-1} in DMSO), with no significant effect on turnover (0.003 s^{-1}). Again, these data are fully consistent with ERK and DMSO functioning to facilitate the enzymatic reaction by stabilizing the active conformation of the general acid loop, but in this case without the aid of general acid catalysis due to the loss of Asp-262. To provide additional evidence that a major portion of the residual activation by DMSO was the direct effect of increased phosphate oxyanion affinity by the activated form, the K_i value of D262N for phosphate was determined in the presence of 25% DMSO. The K_i value was 3.29 ± 0.99 mM and 4.3-fold lower than in the absence of DMSO, consistent with the idea that both DMSO and ERK are functioning, in part, to allow tighter substrate/ligand binding.

Inability of D262N To Readily Dephosphorylate Diphosphorylated ERK. Our results provide strong evidence that D262N is the bona fide general acid residue, and that the D262N enzyme is still capable of significant activation by ERK through the tighter binding of substrate and partial transition state stabilization from Arg-299 and/or Asn-262. These effects are manifested through the proper positioning of the general acid loop, where the carbonyl oxygen of Ile-260 is hydrogen-bonded to the active site Arg-299 (Scheme 2). The X-ray structure of the Pyst1 catalytic domain had revealed an open and presumably inactive conformation of the phosphatase (*18*). Asp-262 of the putative general acid loop was found to be 20 Å away from a position that would

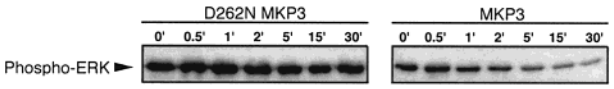

FIGURE 6: Dephosphorylation of phosphorylated ERK by MKP3 and the D262N mutant. Recombinant phosphorylated ERK (*32*) at a final concentration of 1 μM was combined with 2 μM recombinant wild-type MKP3 or MKP3 mutant D262N in 20 mM HEPES, pH 7.4, containing 10 mM $MgCl_2$. Reactions were incubated at 30 °C for the indicated times prior to quenching. The phosphorylation state of ERK was determined using SDS−PAGE and western analysis with an antibody that recognizes diphosphorylated ERK (*32*).

be required for participation in catalysis. Likely as a result of the open conformation and the inability of the carbonyl oxygen of Ile-260 to now hydrogen bond to the active site Arg-299, the arginine residue is improperly positioned to function in phosphate binding. When properly activated, MKP3 exhibits efficient general acid catalysis (*13*). Here we demonstrate that the D262N mutant cannot provide general acid catalysis. As predicted with artificial substrates, the effect of the D262N mutation on k_3 becomes vanishingly small as the pK_a of the leaving group oxygen is lowered. Inversely, as the pK_a is elevated, the D262N enzyme becomes increasingly poorer than wild type. By a pK_a of 7.8, activated D262N is 80-fold worse than activated wild-type MKP3. This would be expected since leaving groups with lower pK_a values are better leaving groups, decreasing the activation energy required in the transition state for phosphoenzyme formation. Unfortunately, for reasons of inherent limitations based on the rate-limiting steps of the enzymatic reaction, the k_3 rate constant for high leaving group pK_a values cannot be ascertained from stopped-flow analysis. Regardless, we can predict that with physiological substrates (phosphotyrosine and phosphothreonine) whose pK_a values are >10 (Figures 2 and 5), the D262N mutant would be more than 1000-fold slower than wild-type MKP3, if D262 is truly playing the role as general acid catalyst. To examine the ability of the D262N mutant to dephosphorylate ERK protein, wild-type or D262N enzymes were reacted with diphosphorylated ERK, and the ability to dephosphorylate this physiological substrate was assessed (Figure 6). At times up to 30 min, the amount of diphosphorylated ERK remaining was determined by western blot analysis using an antibody that recognizes the diphosphorylated form of ERK. As is clearly evident from the blot (Figure 6), the D262N mutant exhibited no detectable dephosphorylation, while the wild-type enzyme displayed dephosphorylation efficiencies similar to those described previously (*32*). The inability of the D262N mutant to efficiently catalyze phosphotyrosine and phosphothreonine hydrolysis is consistent with the loss of general acid catalysis and with D262 playing an essential role in donating its proton to the leaving group oxygen in the transition state for P−O cleavage (Scheme 2).

Background on Kinetic Isotope Effects and PTP Transition State Analysis. The kinetic isotope effects yield information about the structure of the transition state for phosphoryl transfer. The transition state for hydrolysis reactions of phosphate monoesters in solution can be described as very loose or "dissociative" in nature, characterized by extensive bond cleavage to the leaving group, minimal bond formation to the nucleophile, and in which the transferring phosphoryl group resembles metaphosphate ion [for reviews, see (*41, 42*) and references cited therein]. Phosphodiesters and

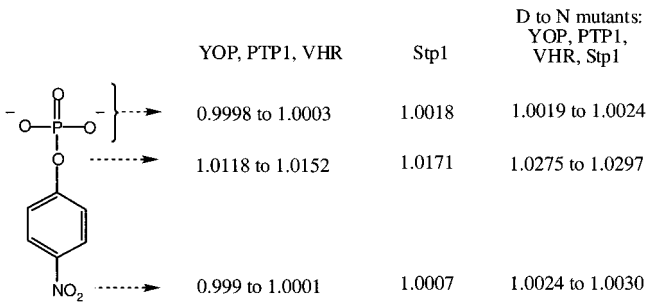

FIGURE 7: Previously reported isotope effects for the DSP VHR and for members of the PTP family, native enzymes (left) and their general acid mutants (right). The diagram of the *p*-nitrophenyl phosphate substrate shows the positions at which isotope effects were measured, where the top arrow is $^{18}(V/K)_{nonbridge}$, the middle arrow is $^{18}(V/K)_{bridge}$, and the bottom arrow is $^{15}(V/K)$. Nomenclature is described under Materials and Methods.

triesters exhibit successively tighter, more associative transition states where the transferring phosphoryl group resembles a pentacoordinate phosphorane (*42*).

Calculations predict inverse nonbridge ^{18}O isotope effects for dissociative transition states, and normal values for associative transition states (*43*). The experimental nonbridge ^{18}O isotope effects for uncatalyzed reactions of the *p*NPP monoester are small and inverse (0.9994−0.9997), while the nonbridge ^{18}O isotope effects for diesters and triesters which have been measured are (with a single exception, which may be anomalous) normal (1.0040−1.0250).

The $^{15}(V/K)$ isotope effect measures charge delocalization in the leaving group, and $^{18}(V/K)_{bridge}$ is an indicator of P−O bond cleavage. The extensive bond cleavage in transition states of reactions of the *p*NPP dianion results in bridge−^{18}O isotope effects of from 1.0202 to 1.030; the resulting development of nearly a full negative charge on the leaving group results in ^{15}N isotope effects of from 1.0028 to 1.0039. When protonation of the leaving group occurs in the transition state, the normal $^{18}(V/K)_{bridge}$ isotope effect arising from P−O bond cleavage is reduced by the inverse isotope effect arising from protonation. This is clearly observed by comparing the uncatalyzed reaction of the *p*NPP monoanion with that of the dianion. During hydrolysis of the monoanion, the leaving group becomes protonated in the transition state, while in the reaction of the dianion, the leaving group departs as the *p*-nitrophenolate anion. Compared to their values in the dianion reaction, the ^{15}k isotope effect is nearly completely abolished in the hydrolysis of the monoanion, and the $^{18}k_{bridge}$ isotope effect is significantly diminished (*31*).

Isotope effect data have been obtained for the native VHR and for its general acid mutant (*25*), as well as for several members of the PTP family (*44, 45*). These data are summarized in Figure 7.

Comparisons of the isotope effects for reactions catalyzed by these native enzymes with data from their general acid mutants reveal a change from a leaving group that is protonated in the transition state to reactions in which the leaving group leaves as the anion in the general acid mutants-(*25, 31, 45*). These general acid mutants also typically exhibit small normal values for $^{18}(V/K)_{nonbridge}$, indicative of increased nucleophilic participation in the transition state. The phosphatase Stp1 exhibits kinetic isotope effects indicative of slightly less efficient protonation of the leaving group in the transition state. The small normal $^{15}(V/K)$ and the slightly

Table 1: Isotope Effects from Reactions of *p*NPP with Native MKP3 and D262N Mutant, in the Presence and Absence of ERK[a]

enzyme	$^{15}(V/K)$	$^{18}(V/K)_{bridge}$	$^{18}(V/K)_{nonbridge}$
native MKP3 with ERK	1.0004 (1)	1.0168 (5)	1.0006 (3)
native MKP3 without ERK	1.0008 (1)	1.0202 (04)	1.0012 (5)
D262N with ERK	1.0031 (4)	1.0316 (13)	1.0023 (6)
D262N without ERK	1.0027 (4)	1.0320 (30)	1.0023 (6)

[a] The standard errors in the last decimal places are given in parentheses.

higher value for $^{18}(V/K)_{bridge}$ both indicate that proton transfer lags slightly behind P−O bond cleavage.

The maximum $^{18}(V/K)_{bridge}$ effect seen in reactions of *p*NPP in solution in which the leaving group is not protonated is around 1.03, and the same value is observed in VHR and in PTPases (including Stp1)when general acid catalysis has been eliminated by mutation (*25, 45*). The equilibrium ^{18}O isotope effect for protonation of *p*-nitrophenol is 0.985 (*31*). Thus, when P−O bond cleavage and proton transfer are both extensive and synchronous, the observed $^{18}(V/K)_{bridge}$ isotope effect should be close to the product of these values, or about 1.015. This is close to the value measured in reactions of *p*NPP with native VHR and with PTP where protonation of the leaving group occurs in the transition state (*25, 45*).

Analysis of MKP3 and D262N by Kinetic Isotope Effects. Within the framework of this background data for related enzymatic reactions, the isotope effects for the MKP3 phosphatase in the present study can be evaluated for the effect of ERK and of the D262N mutation on the transition state of the phosphoryl transfer reaction. The isotope effect data with their standard errors for the reactions of the native MKP3 and the D262N mutant, with and without ERK, are shown in Table 1. The $^{18}(V/K)_{nonbridge}$ values shown are the isotope effects resulting from ^{18}O in all three nonbridge oxygen atoms.

The patterns of the three isotope effects for the reaction with native MKP3 in the presence of ERK are indicative of a reaction where the leaving group is protonated in the transition state. Protonation may be slightly behind P−O bond cleavage, as all three isotope effects lie between those typical of native VHR and PTPs, and those observed for Stp1. Consistent with less efficient general acid catalysis with MKP3 alone, the degree of proton transfer to the leaving group inferred from the data is slightly less in the absence of ERK. However, when ERK is absent, the isotope effects are not as different as would be expected if the absence of ERK completely disables general acid catalysis. The transition state in this case closely resembles that of the reaction in the presence of ERK. The possibility that general acid catalysis is lost but a commitment factor is significantly suppressing the isotope effects from their true values can be ruled out. If this were the case, all of the isotope effects would be reduced from their intrinsic values by the same proportion. Since the maximum value for $^{18}(V/K)_{bridge}$ when general acid catalysis is lost is about 1.03, if one assumes that the intrinsic value for $^{18}(V/K)_{bridge}$ for the reaction of native MKP3 without ERK is actually this value, then the intrinsic value for $^{15}(V/K)$ would be 1.0012, less than half its predicted value if general acid catalysis is indeed inoperative.

One explanation for the isotope effects observed of the native MKP3 would suggest that when ERK is absent, the reaction proceeds through a transition state in which proton transfer to the leaving group is similar but not quite as complete as in the wild type. However, this explanation does not explain the large difference in rate imparted by ERK; the difference in the degree of proton transfer in the transition state implied by the KIEs would seem too little to account for a significant difference in rates.

A more likely possibility is a situation in which ERK facilitates general acid catalysis, but in the absence of ERK, most of MKP3 is in an inactive (or much less active) state, in which movement of the loop enabling general acid catalysis is not efficient (Scheme 2). It is possible that in the absence of ERK, slow reaction takes place from the small amount of active form of the enzyme, in which general acid catalysis still operates, but much more slowly than when ERK is present. Under these conditions, some fraction of the reaction may take place from a form of the enzyme in which general acid catalysis is inoperative, in which case the observed KIEs would be the weighted average of the two reactions. In other words, ERK binding facilitates movement of the loop with the general acid; however, when ERK is not present, loop movement can still occur, but very inefficiently. Hence, a much slower rate of reaction is observed, but one in which the transition state looks essentially the same as when ERK is present. With a labile substrate like *p*NPP, we may also get some slow reaction of bound substrate proceeding without general acid assistance. It should be noted that the D262N mutant exhibits a rate for V/K only 2.3-fold slower (with *p*NPP) than the native enzyme (in the absence of ERK).

In the reactions of the D262N mutant, the KIEs are all typical of the pattern seen when general acid catalysis is lost, and the leaving group departs as the phenolate anion (Table 1). The isotope effects are within experimental error of one another in the presence and in the absence of ERK. This is clear confirmation of the role of D262N as a general acid in the phosphoryl transfer from substrate to the active site cysteine residue.

It is intriguing to note that ERK activation of MKP3 appears to have a relatively small effect on the ability of the enzyme to catalyze hydrolysis of the phospho-enzyme intermediate (k_5). While the rate enhancement with wild-type enzyme was at most 5−6-fold (*13*), the D262N mutant displayed no activation on this step (Figure 3). In fact, the D262N enzyme displayed a slightly lower k_5 value in the presence of ERK compared with free D262N (values below pK_a of 7 in Figure 3). Together these data suggest that ERK may not play an essential role in activating this catalytic step. More importantly though, the data clearly indicate that D262 is functioning during intermediate hydrolysis whether ERK is present, contributing ∼20-fold rate enhancement in MKP3 alone and as much as ∼80-fold in ERK-activated MKP3. It has been previously proposed that Asp-92 in VHR is functioning as a general base during intermediate hydrolysis, activating a water molecule for direct attack on the thiol−phosphate intermediate (*39*). Similarly, we propose that Asp-262 is facilitating this step by functioning as a general base catalyst. When this residue is replaced with Asn, the presence of ERK has no bearing on rate enhancement for this step. This implies that the general acid loop is already properly positioned in the closed conformation, and that Arg-299 is correctly aligned within the active site by Ile-260 of the

general acid loop. An argument can be made that ERK association and subsequent activation is only required during the formation of the phospho-enzyme intermediate. Once formed, intermediate hydrolysis can proceed without the need for ERK stabilization of the active conformation. This idea begs other intriguing questions on the mechanism of dephosphorylation. Specifically, does MKP3 dephosphorylate phosphorylated ERK (pERK) within the same complex (intramolecular) or does the activated ERK−MKP3 complex dephosphorylate a separate molecule of pERK (intermolecular)? If an intramolecular mechanism is operating, then dephosphorylated ERK must be released from MKP3 after catalysis and prior to binding the next pERK molecule. This is an especially important point since it has been observed that pERK and ERK can bind to the N-terminal domain of MKP3. Unfortunately, the relative binding affinities have not been determined. In the intramolecular mechanism, release of dephosphorylated ERK after intermediate formation would be a logical step in which to release the protein product. In contrast, an intermolecular mechanism would only require initial N-terminal binding of ERK (either pERK or ERK) and subsequent phosphatase activation. This ERK−MKP3 complex need not dissociate, but instead acts as the active enzyme species toward additional pERK molecules, via active site interactions. We are currently pursuing these critical mechanistic questions.

REFERENCES

1. Keyse, S. M. (2000) *Curr. Opin. Cell Biol. 12* (2), 186−192.
2. Robinson, M. J., and Cobb, M. H. (1997) *Curr. Opin. Cell Biol. 9* (2), 180−186.
3. Ip, Y. T., and Davis, R. J. (1998) *Curr. Opin. Cell Biol. 10* (2), 205−219.
4. Sun, H., Charles, C. H., Lau, L. F., and Tonks, N. K. (1993) *Cell 75* (3), 487−493.
5. Ward, Y., Gupta, S., Jensen, P., Wartmann, M., Davis, R. J., and Kelly, K. (1994) *Nature 367* (6464), 651−654.
6. Kwak, S. P., and Dixon, J. E. (1995) *J. Biol. Chem. 270* (3), 1156−1160.
7. Groom, L. A., Sneddon, A. A., Alessi, D. R., Dowd, S., and Keyse, S. M. (1996) *EMBO J. 15* (14), 3621−3632.
8. Muda, M., Boschert, U., Dickinson, R., Martinou, J. C., Martinou, I., Camps, M., Schlegel, W., and Arkinstall, S. (1996) *J. Biol. Chem. 271* (8), 4319−4326.
9. Chu, Y., Solski, P. A., Khosravi-Far, R., Der, C. J., and Kelly, K. (1996) *J. Biol. Chem. 271* (11), 6497−6591.
10. Hirsch, D. D., and Stork, P. J. (1997) *J. Biol. Chem. 272* (7), 4568−4575.
11. Mourey, R. J., Vega, Q. C., Campbell, J. S., Wenderoth, M. P., Hauschka, S. D., Krebs, E. G., and Dixon, J. E. (1996) *J. Biol. Chem. 271* (7), 3795−3802.
12. Camps, M., Nichols, A., Gillieron, C., Antonsson, B., Muda, M., Chabert, C., Boschert, U., and Arkinstall, S. (1998) *Science 280* (5367), 1262−1265.
13. Fjeld, C. C., Rice, A. E., Kim, Y., Gee, K. R., and Denu, J. M. (2000) *J. Biol. Chem. 275* (10), 6749−6757.
14. Camps, M., Nichols, A., and Arkinstall, S. (2000) *FASEB J. 14* (1), 6−16.
15. Nichols, A., Camps, M., Gillieron, C., Chabert, C., Brunet, A., Wilsbacher, J., Cobb, M., Pouyssegur, J., Shaw, J. P., and Arkinstall, S. (2000) *J. Biol. Chem. 275* (32), 24613−24621.
16. Zhou, B., Wu, L., Shen, K., Zhang, J., Lawrence, D. S., and Zhang, Z. Y. (2001) *J. Biol. Chem. 276*, (9), 6506−6515.
17. Tanoue, T., Adachi, M., Moriguchi, T., and Nishida, E. (2000) *Nat. Cell Biol. 2* (2), 110−116.
18. Stewart, A. E., Dowd, S., Keyse, S. M., and McDonald, N. Q. (1999) *Nat. Struct. Biol. 6* (2), 174−181.
19. Yuvaniyama, J., Denu, J. M., Dixon, J. E., and Saper, M. A. (1996) *Science 272* (5266), 1328−1331.
20. Zhou, G., Denu, J. M., Wu, L., and Dixon, J. E. (1994) *J. Biol. Chem. 269* (45), 28084−28090.
21. Denu, J. M., Zhou, G., Wu, L., Zhao, R., Yuvaniyama, J., Saper, M. A., and Dixon, J. E. (1995) *J. Biol. Chem. 270* (8), 3796−3803.
22. Denu, J. M., Zhou, G., Guo, Y., and Dixon, J. E. (1995) *Biochemistry 34* (10), 3396−3403.
23. Denu, J. M., Stuckey, J. A., Saper, M. A., and Dixon, J. E. (1996) *Cell 87* (3), 361−364.
24. Denu, J. M., and Dixon, J. E. (1995) *Proc. Natl. Acad. Sci. U.S.A. 92* (13), 5910−5914.
25. Hengge, A. C., Denu, J. M., and Dixon, J. E. (1996) *Biochemistry 35* (22), 7084−7092.
26. Zhou, B., and Zhang, Z. Y. (1999) *J. Biol. Chem. 274* (50), 35526−35534.
27. Chen, W., Wilborn, M., and Rudolph, J. (2000) *Biochemistry 39* (35), 10781−10789.
28. Wiland, A. M., Denu, J. M., Mourey, R. J., and Dixon, J. E. (1996) *J. Biol. Chem. 271* (52), 33486−33492.
29. Robbins, D. J., Zhen, E., Owaki, H., Vanderbilt, C. A., Ebert, D., Geppert, T. D., and Cobb, M. H. (1993) *J. Biol. Chem. 268* (7), 5097−5106.
30. Gee, K. R., Sun, W. C., Bhalgat, M. K., Upson, R. H., Klaubert, D. H., Latham, K. A., and Haugland, R. P. (1999) *Anal. Biochem. 273* (1), 41−48.
31. Hengge, A. C., Edens, W. A., and Elsing, H. (1994) *J. Am. Chem. Soc. 116*, 5045−5049.
32. Todd, J. L., Tanner, K. G., and Denu, J. M. (1999) *J. Biol. Chem. 274*, 13271−13280.
33. Bigeleisen, J., and Wolfsberg, M. (1958) *Adv. Chem. Phys. 1*, 15−76.
34. O'Leary, M. H., and Marlier, J. F. (1979) *J. Am. Chem. Soc. 101*, 3300−3306.
35. Caldwell, S. R., Raushel, F. M., Weiss, P. M., and Cleland, W. W. (1991) *Biochemistry 30*, 7444−7450.
36. Northrop, D. B. (1977) *Isotope Effects on Enzyme-Catalyzed Reactions* (Cleland, W. W., O'Leary, M. H., and Northrop, D. B., Eds.) University Park Press, Baltimore, MD.
37. Denu, J. M., and Dixon, J. E. (1998) *Curr. Opin. Chem. Biol. 2* (5), 633−641.
38. Denu, J. M., Stuckey, J. A., Saper, M. A., and Dixon, J. E. (1996) *Cell 87* (3), 361−364.
39. Denu, J. M., Lohse, D. L., Vijayalakshmi, J., Saper, M. A., and Dixon, J. E. (1996) *Proc. Natl. Acad. Sci. U.S.A. 93* (6), 2493−2498.
40. Hoff, R. H., Hengge, A. C., Wu, L., Keng, Y. F., and Zhang, Z. Y. (2000) *Biochemistry 39* (1), 46−54.
41. Hengge, A. C. (1998) *Comprehensive Biological Catalysis: A Mechanistic Reference* (Sinnott, M., Ed.) Vol. 1, Academic Press, San Diego, CA.
42. Thatcher, G. R. J., and Kluger, R. (1989) *Adv. Phys. Org. Chem. 25*, 99−265.
43. Weiss, P. M., Knight, W. B., and Cleland, W. W. (1986) *J. Am. Chem. Soc. 108*, 2761−2762.
44. Hengge, A. C., Sowa, G. A., Wu, L., and Zhang, Z. Y. (1995) *Biochemistry 34* (43), 13982−13987.
45. Hengge, A. C., Zhao, Y., Wu, L., and Zhang, Z. Y. (1997) *Biochemistry 36* (25), 7928−7936.

BI002951V